https://doi.org/10.5194/egusphere-2026-3994
Preprint. Discussion started: 5 August 2026

Fractal Rupture Geometry and Nonlinear Stress-Drop Scaling in Earthquake Source Parameters

Antonino D'Alessandro
Istituto Nazionale di Geofisica e Vulcanologia, Osservatorio Nazionale Terremoti, Rome, Italy
antonino.dalessandro@ingv.it
https://orcid.org/0000-0002-0074-3125

Abstract

Static stress drop is commonly interpreted within a Euclidean self-similar rupture framework in which rupture area scales as $A \propto L^2$, seismic moment scales as $M_0 \propto L^3$, and stress drop is independent of earthquake size. Here, I develop and test an alternative geometrical scaling framework in which the effective rupture support is non-Euclidean and scales as $A_{\mathrm{eff}} \propto L^{D_f}$, with $2 < D_f < 3$. For self-similar slip, this assumption predicts a power-law stress-drop scaling, $\Delta\sigma \propto M_0^{\beta}$, with $\beta = (D_f - 2)/(D_f + 1)$, thereby linking an observable source-scaling exponent to an equivalent effective rupture-support dimension. Synthetic tests show that weak positive exponents in the theoretically predicted range are recoverable under realistic lognormal scatter. The framework is then applied to an open source-parameter catalog from the Southeastern Alps, using 1521 earthquakes with finite positive seismic moment and static stress drop. The full-catalog log–log regression gives $\hat{\beta}_{\mathrm{obs}} = 0.223$, with bootstrap median 0.222 and 95 % confidence interval [0.180, 0.263]. A binned-median regression gives a consistent exponent of approximately 0.192. Under self-similar slip, the observed exponent maps to an equivalent rupture-support dimension $D_f^{\mathrm{eq}} \simeq 2.86$, with an observationally compatible range approximately $[2.66, 3^{-}]$. Moment-threshold tests, residual diagnostics, and leave-one-block-out jackknife analyses indicate that the positive scaling is stable within the analyzed catalog. These results do not constitute direct evidence that earthquake ruptures are fractal objects. Rather, they show that a non-Euclidean effective rupture-support framework provides a mathematically derived, observationally compatible, and testable explanation for positive stress-drop scaling in a regional source-parameter catalog.

https://doi.org/10.5194/egusphere-2026-3994
Preprint. Discussion started: 5 August 2026

1 Introduction

Static stress drop is a central source parameter in earthquake physics because it links seismic moment, source dimension, and the intensity of coseismic stress release. In the classical self-similar framework, earthquake rupture is assumed to occur on a smooth Euclidean fault support whose area scales as $A \propto L^2$. If average slip scales linearly with rupture length, $\bar{u} \propto L$, seismic moment scales as $M_0 \propto L^3$, and stress drop is expected to be independent of earthquake size. This constant-stress-drop limit is deeply embedded in classical earthquake source theory and in the interpretation of source spectra (Aki, 1967; Brune, 1970; Kanamori and Anderson, 1975).

Despite its conceptual simplicity, the constant-stress-drop paradigm remains debated. Empirical stress-drop estimates commonly display substantial scatter, and their dependence on seismic moment is sensitive to source-model assumptions, corner-frequency estimation, attenuation correction, finite bandwidth, path and site effects, and catalog selection. Some studies support approximate self-similarity over broad magnitude ranges, whereas others report systematic stress-drop variability with magnitude, depth, tectonic setting, or rupture environment (Abercrombie, 1995; Ide and Beroza, 2001; Allmann and Shearer, 2009). This ambiguity has two implications. First, apparent stress-drop scaling cannot be interpreted without careful attention to methodological bias. Second, if a stable scaling exponent is recovered from an internally homogeneous source-parameter catalog, it may contain information about source physics beyond the classical Euclidean approximation.

A key limitation of the classical argument is that it assumes a smooth rupture support with Euclidean area–length scaling. Natural fault zones, however, are geometrically complex. Fault surfaces and fault traces exhibit roughness, segmentation, branching, anisotropic topography, and scale-dependent structural organization over finite observational ranges (Brown and Scholz, 1985; Power et al., 1987; Okubo and Aki, 1987; Candela et al., 2012; Brodsky et al., 2016). Such geometrical complexity need not imply that earthquake ruptures occupy a truly volumetric domain, nor that natural faults are ideal mathematical fractals across all scales. It does, however, motivate a more general scaling question: if the effective rupture support activated during an

https://doi.org/10.5194/egusphere-2026-3994
Preprint. Discussion started: 5 August 2026

earthquake does not scale as a smooth Euclidean area, how should static stress drop scale with seismic moment?

This study addresses that question by developing a geometrical rupture-scaling framework in which the active rupture support has an effective dimension D_f, with $2 < D_f < 3$. The central hypothesis is that the effective support involved in moment release scales as $A_{\mathrm{eff}} \propto L^{D_f}$, rather than $A \propto L^2$. Under self-similar slip, this assumption yields a direct analytical prediction linking the stress-drop scaling exponent β to the effective rupture-support dimension, $\beta = (D_f - 2)/(D_f + 1)$. The Euclidean limit $D_f = 2$recovers $\beta = 0$, whereas $D_f > 2$ predicts weak but positive stress-drop scaling, $\Delta\sigma \propto M_0^{\beta}$. The conceptual structure of the framework is summarized in Fig. 1, which contrasts the Euclidean planar limit with an effective geometrically complex rupture support and its observable stress-drop consequence.

The objective of this paper is not to claim that earthquake ruptures are directly observed as fractal objects. Instead, I test whether a non-Euclidean effective rupture-support scaling provides a physically consistent explanation for positive stress-drop scaling in an open source-parameter catalog. The distinction is important. The dimension inferred from stress-drop scaling is an equivalent, model-dependent quantity; it is not an independent geometrical measurement of a fault surface. Accordingly, I interpret $D_f$as an effective rupture-support dimension that parameterizes the scaling of geometrically active source support with earthquake size.

The observational test uses an open catalog of source parameters for earthquakes in the Southeastern Alps. This catalog is suitable because it reports seismic moment and static stress drop directly, avoiding the need to infer M_0 from heterogeneous magnitude proxies. The analysis estimates the first-order $\Delta\sigma$–M_0 scaling exponent, evaluates its uncertainty by bootstrap resampling, tests the recoverability of weak positive exponents using synthetic catalogs, and assesses robustness with moment-threshold sensitivity, residual diagnostics, and leave-one-block-out jackknife tests.

The paper is organized as follows. Section 2 derives the theoretical scaling relations for Euclidean and non-Euclidean rupture supports. Section 3 describes the open source-parameter catalog and the variables used in the analysis. Section 4 presents the regression, bootstrap, synthetic, binning, and robustness procedures. Section 5 reports the theoretical, synthetic, and observational results. Section 6 discusses the physical

https://doi.org/10.5194/egusphere-2026-3994
Preprint. Discussion started: 5 August 2026

interpretation, limitations, alternative explanations, and implications for stress-drop scaling. Section 7 summarizes the main conclusions.

2 Theoretical framework

Classical earthquake source scaling is commonly formulated by assuming that rupture occurs on a smooth Euclidean fault support with characteristic linear dimension L. For a planar rupture, the rupture area scales as

$$A \propto L^2. \qquad (1)$$

The scalar seismic moment is

$$M_0 = \mu A \bar{u}, \qquad (2)$$

where μ is the shear modulus and $\bar{u}$ is the average coseismic slip. Under self-similar slip scaling,

$$\bar{u} \propto L, \qquad (3)$$

Eqs. (1)–(3) imply

$$M_0 \propto L^3. \qquad (4)$$

For standard crack-like source models, static stress drop can be expressed, up to geometry-dependent constants, as

$$\Delta\sigma \propto \frac{M_0}{L^3}. \qquad (5)$$

https://doi.org/10.5194/egusphere-2026-3994
Preprint. Discussion started: 5 August 2026

Combining Eqs. (4) and (5) gives

$$\Delta\sigma \propto L^0 = \text{const.} \qquad (6)$$

Equations (1)–(6) define the Euclidean self-similar limit: seismic moment increases as L^3, whereas static stress drop remains scale invariant. This limit is the appropriate null model for the present analysis and is consistent with classical earthquake source theory, in which source spectra, moment scaling, and stress-drop estimates are interpreted under self-similar rupture assumptions (Aki, 1967; Brune, 1970; Kanamori and Anderson, 1975). The corresponding conceptual geometry is illustrated in Fig. 1a.

I generalize Eq. (1) by replacing the Euclidean rupture area $A$with an effective rupture support A_{eff}. The central assumption is that the measure of the active rupture support scales with source size as

$$A_{\text{eff}} \propto L^{D_f},\ 2 < D_f < 3. \qquad (7)$$

The exponent D_f is interpreted as an effective rupture-support dimension. It does not imply that the earthquake rupture occupies a volumetric domain in a literal topological sense. Rather, it parameterizes how the geometrically active rupture support increases with L when rupture involves segmentation, roughness, distributed activation, or multiscale structural complexity. In this sense, D_f is a scaling descriptor of the effective source support, not a direct observation of the fractal dimension of a mapped fault surface.

This distinction is essential because natural faults display roughness, segmentation, and scale-dependent geometrical complexity over finite observational ranges, but these properties do not by themselves imply that every earthquake rupture realizes an ideal mathematical fractal. Previous studies of fault roughness and fault-system geometry have documented fractal or self-affine characteristics of natural fault surfaces and fault traces (Power et al., 1987; Okubo and Aki, 1987; Brown and Scholz, 1985). The present framework uses this geometrical perspective only in an effective scaling sense: over the moment range sampled by a source-parameter catalog, the active rupture support may depart from the Euclidean relation $A \propto L^2$. The conceptual contrast between the Euclidean and geometrically complex cases is shown in Fig. 1a,b.

https://doi.org/10.5194/egusphere-2026-3994
Preprint. Discussion started: 5 August 2026

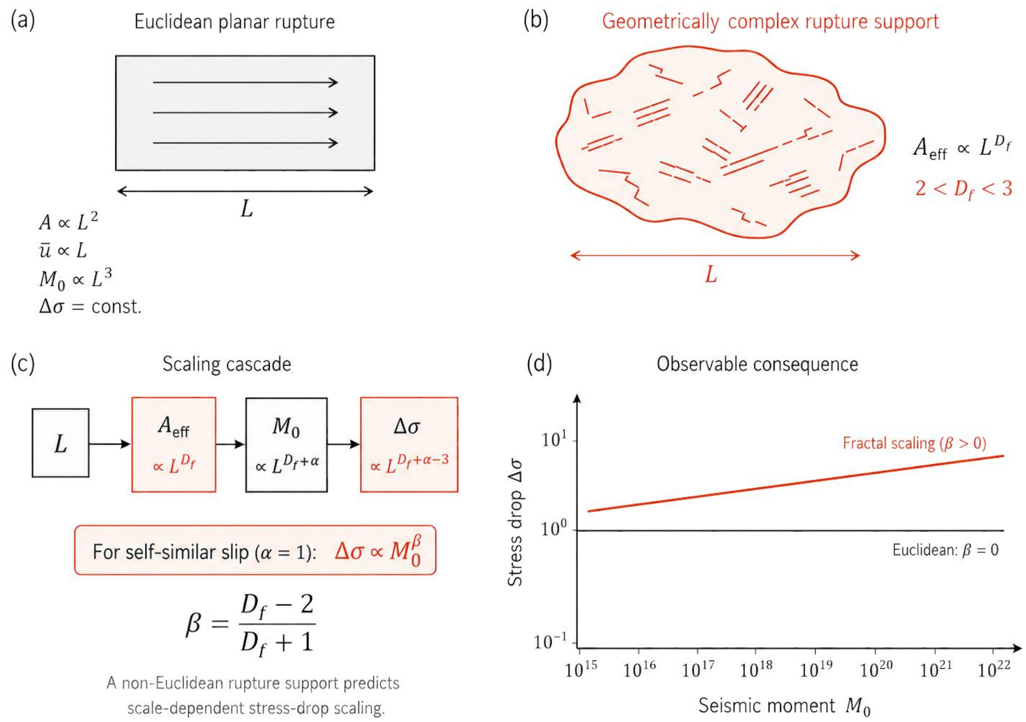

Figure 1. *Conceptual framework linking rupture-support geometry to stress-drop scaling. (a) Euclidean planar rupture model. A smooth planar support implies $A \propto L^2$; for self-similar slip, $\bar{u} \propto L$, the seismic moment scales as $M_0 \propto L^3$, yielding scale-invariant stress drop. (b) Non-Euclidean effective rupture support. Geometrical complexity, segmentation, and roughness are represented through an effective support whose measure scales as $A_{eff} \propto L^{D_f}$, with $2 < D_f < 3$. Here D_f denotes an effective rupture-support dimension, not a directly observed volumetric rupture dimension. (c) Scaling cascade from rupture length to effective support, seismic moment, and stress drop. For general slip scaling $\bar{u} \propto L^\alpha$, the model gives $M_0 \propto L^{D_f+\alpha}$ and $\Delta\sigma \propto L^{D_f+\alpha-3}$. For self-similar slip $(\alpha = 1)$, this reduces to $\Delta\sigma \propto M_0^\beta$, with $\beta = (D_f - 2)/(D_f + 1)$. (d) Observable consequence in $\Delta\sigma$–M_0 space. The Euclidean limit predicts $\beta = 0$, whereas a geometrically complex effective rupture support predicts positive stress-drop scaling $(\beta > 0)$.*

To retain generality, the average slip is allowed to scale as

https://doi.org/10.5194/egusphere-2026-3994
Preprint. Discussion started: 5 August 2026

$$\bar{u} \propto L^{\alpha}, \qquad (8)$$

where $\alpha = 1$ recovers self-similar slip. Substituting Eqs. (7) and (8) into the seismic moment definition gives

$$M_0 \propto \mu A_{\mathrm{eff}} \bar{u} \propto L^{D_f+\alpha}. \qquad (9)$$

Using the first-order stress-drop scaling in Eq. (5), the corresponding stress-drop dependence on source size becomes

$$\Delta\sigma \propto \frac{M_0}{L^3} \propto L^{D_f+\alpha-3}. \qquad (10)$$

Equations (7)–(10) define the scaling cascade summarized in Fig. 1c. Eliminating Lbetween Eqs. (9) and (10) yields a power-law relation between static stress drop and seismic moment,

$$\Delta\sigma \propto M_0^{\beta}, \qquad (11)$$

where

$$\beta = \frac{D_f + \alpha - 3}{D_f + \alpha}. \qquad (12)$$

Equation (12) is the general theoretical prediction of the framework. It shows that positive stress-drop scaling may arise from a non-Euclidean effective rupture support, from non-self-similar slip scaling, or from a combination of both. Therefore, an observed positive β cannot be interpreted uniquely as a direct measurement of D_f unless an explicit assumption about $\alpha$is imposed.

For the self-similar slip case,

https://doi.org/10.5194/egusphere-2026-3994
Preprint. Discussion started: 5 August 2026

$$\alpha = 1, \qquad (13)$$

Eq. (12) reduces to

$$\beta = \frac{D_f - 2}{D_f + 1}. \qquad (14)$$

This expression has three relevant limiting properties. First, the Euclidean limit $D_f = 2$ gives

$$\beta = 0, \qquad (15)$$

which recovers scale-invariant stress drop. Second, for $2 < D_f < 3$,

$$0 < \beta < \frac{1}{4}. \qquad (16)$$

Thus, even relatively strong departures from Euclidean rupture-support scaling produce only moderate positive values of β. Third, $\beta(D_f)$ is monotonic, so larger effective rupture-support dimensions correspond to larger positive stress-drop scaling exponents. This theoretical mapping is shown in Fig. 2, where the Euclidean case defines the horizontal constant-stress-drop reference and increasing D_f produces progressively steeper $\Delta\sigma$–M_0 scaling.

https://doi.org/10.5194/egusphere-2026-3994
Preprint. Discussion started: 5 August 2026

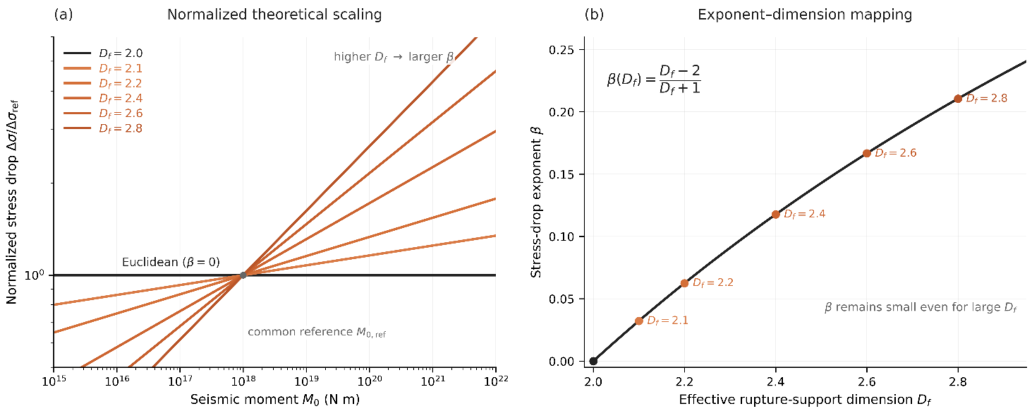

Figure 2. *Theoretical stress-drop scaling predicted by the effective rupture-support framework. (a) Normalized stress-drop scaling as a function of seismic moment M_0 for different values of the effective rupture-support dimension D_f, assuming self-similar slip ($\alpha = 1$). All curves are normalized at the common reference moment $M_{0,ref}$. The Euclidean case $(D_f = 2)$gives scale-invariant stress drop ($\beta = 0$), whereas increasing $D_f$produces progressively steeper positive scaling. (b) Analytical mapping between the stress-drop exponent $\beta$and the effective rupture-support dimension D_f, given by $\beta(D_f) = (D_f - 2)/(D_f + 1)$. The relation shows that even substantial departures from Euclidean rupture-support scaling produce moderate positive exponents, implying that geometrical complexity can generate systematic but limited deviations from constant stress drop.*

Under the self-similar slip assumption, Eq. (14) can be inverted to express an observed stress-drop exponent as an equivalent rupture-support dimension,

$$D_f^{\mathrm{eq}} = \frac{2 + \beta}{1 - \beta}. \qquad (17)$$

For the more general case in which $\alpha$is not fixed, Eq. (12) gives

https://doi.org/10.5194/egusphere-2026-3994
Preprint. Discussion started: 5 August 2026

$$D_f = \frac{3}{1-\beta} - \alpha. \qquad (18)$$

Equations (17) and (18) clarify the epistemic status of D_f^{eq}. The quantity D_f^{eq} is not an independently observed fractal dimension. It is a model-dependent equivalent dimension obtained by mapping an observed β onto the theoretical relation in Eq. (14). If $\alpha = 1$, D_f^{eq} provides a compact geometrical interpretation of the stress-drop scaling exponent. If $\alpha \neq 1$, the same observed β may reflect a trade-off between rupture-support geometry and slip scaling.

Accordingly, the framework distinguishes between three levels of inference. The consolidated theoretical result is the analytical relation between rupture-support scaling and stress-drop scaling given by Eqs. (12) and (14). A plausible physical interpretation is that a robust positive β reflects increasing effective geometrical complexity of the rupture support with source size. A more speculative interpretation, requiring independent geometrical or finite-source validation, is that D_f^{eq} approximates the fractal dimension of the active rupture network itself.

The framework rests on four assumptions. First, the source can be represented by a characteristic length scale L. Second, the effective rupture support follows a power-law area–length scaling over the sampled moment range. Third, static stress drop is adequately represented, to first order, by M_0/L^3, with geometry-dependent constants affecting the intercept rather than the scaling exponent. Fourth, observational estimates of M_0 and $\Delta\sigma$ are sufficiently homogeneous that a first-order log–log scaling exponent can be estimated meaningfully.

These assumptions define the requirements for observational testing. The source-parameter catalog must contain direct or consistently derived estimates of seismic moment and stress drop. Synthetic tests are required to verify whether weak positive exponents of the magnitude predicted by Eq. (14) can be recovered under realistic scatter. Robustness tests must then evaluate whether the inferred $\hat{\beta}$ is stable with respect to moment threshold, residual structure, and subset selection.

Within these limits, the framework is falsifiable. If rupture geometry is effectively Euclidean and slip scaling is self-similar, then β should be statistically indistinguishable from zero. Conversely, a robust positive β, if not attributable to catalog bias, attenuation effects, finite bandwidth, corner-frequency trade-offs, or regression artifacts, is compatible with non-Euclidean effective rupture-support scaling.

https://doi.org/10.5194/egusphere-2026-3994
Preprint. Discussion started: 5 August 2026

3 Data

I use an open source-parameter catalog for earthquakes that occurred in the Southeastern Alps between 2016 and 2023 (Moratto and Saraò, 2025). The catalog is distributed through Zenodo as an openly accessible spreadsheet dataset and is associated with a companion tectonic interpretation study by Moratto et al. (2026), reported in the dataset metadata as a Tectonophysics article in press. The record describes the dataset as a catalog of source parameters estimated for earthquakes in the Southeastern Alps and explicitly lists moment magnitude M_W, seismic moment M_0, corner frequency f_c, quality factor Q_0, source radius r, static stress drop $\Delta\sigma$, radiated energy E_r, apparent stress, and seismic efficiency among the reported variables.

This catalog is appropriate for the present analysis because it provides the two quantities required by the theoretical framework: seismic moment and static stress drop. I therefore avoid using local magnitude or non-homogenized magnitude proxies to infer M_0, which would introduce an additional source of scaling bias. This point is essential because the objective of the paper is not to derive source parameters from waveform data, but to test whether independently estimated source parameters show the scaling predicted by the fractal rupture-support framework. The source parameters in the catalog were estimated with the SourceSpec software, which derives earthquake source parameters from P- or S-wave displacement spectra (Satriano, 2024). The dataset metadata further specify that parameters averaged across stations were averaged in logarithmic space and that lower and upper uncertainty bounds were reported for parameters such as M_0 and f_c, reflecting asymmetric uncertainty after back-transformation to linear scale.

The observational analysis was restricted to events for which both M_0 and $\Delta\sigma$ were available, finite, and strictly positive. This filtering is required because all scaling estimates are computed in logarithmic space. After data cleaning and filtering, the working catalog contains $N = 1521$events. This retained subset defines the empirical $\Delta\sigma$–M_0 relation used for the observational regression, the binned-median diagnostic, the bootstrap uncertainty analysis, and the robustness tests described below.

The spatial and tectonic setting of the dataset is regional rather than global. Consequently, the observational component of the paper should be interpreted as a regional test of a general theoretical prediction, not as global evidence for universal stress-drop scaling. The Southeastern Alps provide a suitable test case because the

https://doi.org/10.5194/egusphere-2026-3994
Preprint. Discussion started: 5 August 2026

catalog is open, reproducible, and internally homogeneous with respect to the source-parameter estimation workflow. However, the regional nature of the dataset implies that the inferred β_{obs} and the corresponding equivalent dimension D_f^{eq} may reflect the tectonic, structural, and methodological characteristics of this specific source region. This limitation is explicitly addressed in the robustness tests and in the Discussion.

The primary variables used in the analysis are the seismic moment M_0, expressed in N m, and the static stress drop $\Delta\sigma$, expressed in MPa. Moment magnitude M_W, corner frequency f_c, source radius r, and the reported uncertainty fields are retained as auxiliary metadata but are not used as dependent variables in the main regression. The regression model is formulated directly in terms of $M_0$and $\Delta\sigma$, consistent with the theoretical prediction

$$\Delta\sigma \propto M_0^{\beta}. \qquad (19)$$

The use of M_0 rather than magnitude is important because the predicted exponent β is defined with respect to seismic moment. Any conversion from magnitude to moment would impose an additional empirical relation and could distort the inferred scaling if magnitudes were heterogeneous or saturated.

The principal limitations of the dataset are those common to stress-drop catalogs derived from spectral source analysis. Static stress drop is not a direct observable; it depends on estimates of corner frequency, attenuation correction, source model assumptions, frequency bandwidth, station coverage, and path/site effects. These factors can introduce both random scatter and systematic bias in $\Delta\sigma$. The catalog nevertheless remains suitable for the present purpose because the analysis targets a first-order scaling exponent across a consistently processed dataset, rather than absolute stress-drop values for individual earthquakes. To reduce the risk that the inferred scaling is an artifact of sampling or regression choices, the Methods section implements synthetic recovery tests, binned medians, non-parametric bootstrap resampling, moment-threshold sensitivity, residual diagnostics, and leave-one-block-out jackknife tests.

The dataset therefore defines a reproducible observational test of the theoretical framework. It does not by itself establish that earthquake ruptures in the Southeastern Alps are fractal in a direct geometrical sense.

https://doi.org/10.5194/egusphere-2026-3994
Preprint. Discussion started: 5 August 2026

Rather, it allows me to evaluate whether the observed $\Delta\sigma$–M_0 scaling is compatible with the effective rupture-support scaling predicted by Eqs. (14) and (17).

4 Methods

All analyses were performed in logarithmic space because the theoretical framework predicts a power-law relationship between static stress drop and seismic moment. Events were retained only if both M_0 and $\Delta\sigma$ were finite and strictly positive. I defined

$$x_i = \log_{10}\left(\frac{M_{0,i}}{M_{0,\mathrm{ref}}}\right),\ y_i = \log_{10}(\Delta\sigma_i), \qquad (20)$$

where $M_{0,\mathrm{ref}} = 10^{18}$ N m. The reference moment only shifts the regression intercept and does not affect the estimated slope. Static stress drop was expressed in MPa, consistently with the source-parameter catalog. The observational scaling model was then written as

$$y_i = a + \beta x_i + \varepsilon_i, \qquad (21)$$

where a is the intercept, β is the stress-drop scaling exponent, and ε_i represents residual variability due to observational scatter, unmodeled source complexity, and methodological uncertainty in source-parameter estimation.

The primary observational estimate $\hat{\beta}$ was obtained by ordinary least squares regression in the (x_i, y_i) space. The OLS estimator was used because the objective was to quantify the first-order log–log trend of $\Delta\sigma$ conditional on M_0, not to construct a full hierarchical measurement-error model. The fitted slope is

$$\hat{\beta} = \frac{\sum_{i=1}^{N}(x_i - \bar{x})(y_i - \bar{y})}{\sum_{i=1}^{N}(x_i - \bar{x})^2},\ \hat{a} = \bar{y} - \hat{\beta}\bar{x}, \qquad (22)$$

https://doi.org/10.5194/egusphere-2026-3994
Preprint. Discussion started: 5 August 2026

where N is the number of retained events. This regression provides the global estimate of the observational stress-drop scaling exponent.

To evaluate whether weak positive exponents of the amplitude predicted by the theoretical framework are recoverable under realistic scatter, I generated synthetic catalogs following

$$\log_{10}\Delta\sigma_i^{\mathrm{syn}} = a_{\mathrm{syn}} + \beta_{\mathrm{true}}\log_{10}\left(\frac{M_{0,i}^{\mathrm{syn}}}{M_{0,\mathrm{ref}}}\right) + \eta_i, \qquad (23)$$

with

$$\eta_i \sim \mathcal{N}\left(0, \sigma^2_{\log\Delta\sigma}\right). \qquad (24)$$

Synthetic seismic moments were sampled uniformly in $\log_{10}M_0$ over the interval 10^{15}–10^{22} N m. I used $N = 500$ events per synthetic catalog and imposed $\sigma_{\log\Delta\sigma} = 0.20$, representing realistic lognormal scatter in stress-drop estimates. Representative synthetic datasets were generated for $\beta_{\mathrm{true}} = 0.00$, 0.08, and 0.16. Monte Carlo recovery tests were then performed using $N_{\mathrm{MC}} = 500$ realizations for each input exponent. A second synthetic experiment sampled β_{true} over the interval 0.00–0.20 to test the linearity and bias of the recovery. These tests are summarized in Fig. 3 and provide a methodological control on whether the predicted signal is identifiable despite substantial stress-drop scatter.

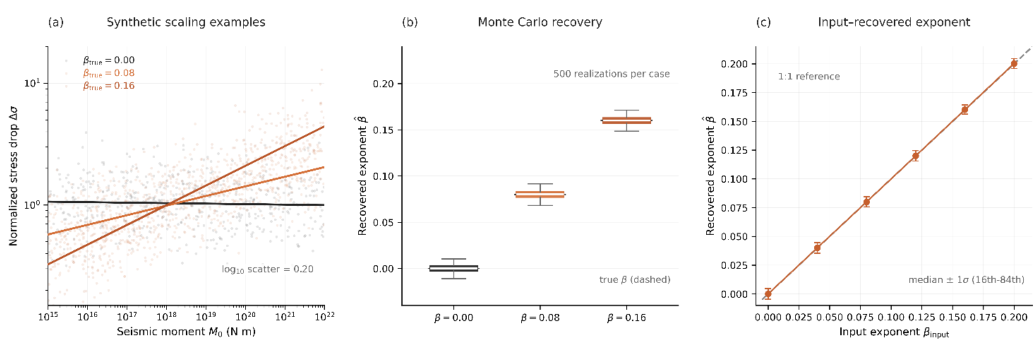

Figure 3. *Synthetic validation of weak stress-drop scaling recovery. (a) Synthetic $\Delta\sigma$–M_0 catalogs generated from prescribed power-law relations $\Delta\sigma \propto M_0^{\beta}$ for representative input exponents. Random lognormal scatter*

https://doi.org/10.5194/egusphere-2026-3994
Preprint. Discussion started: 5 August 2026

is added to reproduce the level of variability expected in stress-drop estimates, and fitted log–log regression lines are shown for comparison. (b) Monte Carlo distributions of recovered scaling exponents $\hat{\beta}$ for repeated synthetic catalogs with different prescribed input values. Dashed horizontal segments indicate the corresponding true exponents. (c) Input–output recovery test showing the median recovered exponent and the 16th–84th percentile range across repeated realizations. The results show that weak positive exponents in the range predicted by the effective rupture-support framework remain statistically recoverable under realistic observational scatter.

For the observational catalog, I quantified uncertainty in $\hat{\beta}_{\mathrm{obs}}$ by non-parametric bootstrap resampling. Each bootstrap replicate was constructed by sampling Nevents with replacement from the cleaned catalog and refitting Eq. (21). I used $N_{\mathrm{boot}} = 1000$ replicates. The bootstrap median was used as the central estimate, and the 2.5th and 97.5th percentiles were used as the 95 % confidence interval. The same bootstrap ensemble was used to map the observational uncertainty in β onto the equivalent rupture-support dimension through

$$D_f^{\mathrm{eq}} = \frac{2+\beta}{1-\beta}. \qquad (25)$$

The bootstrap procedure follows the standard non-parametric resampling logic of Efron (1979). Its use here is descriptive and empirical: it estimates the stability of the fitted scaling exponent under repeated sampling of the available catalog. It does not account for possible spatial or temporal dependence among earthquakes, nor for full covariance between M_0, f_c, source radius, and $\Delta\sigma$. These limitations are considered in the robustness analysis and in the Discussion.

In addition to the event-level OLS fit, I computed binned median stress drop as a function of seismic moment. Events were grouped in logarithmic moment bins, and for each bin I calculated the median $\Delta\sigma$ and the 16th–84th percentile interval. A separate log–log regression was then fitted to the binned medians. This binned estimate was not used as the primary estimator because binning reduces the number of independent points and discards within-bin information. It was instead used as a robustness diagnostic to verify that the inferred

https://doi.org/10.5194/egusphere-2026-3994
Preprint. Discussion started: 5 August 2026

positive scaling was not controlled solely by the high-density portion of the point cloud. The full-catalog fit, binned median trend, bootstrap distribution, and theoretical mapping to D_f^{eq} are reported in Fig. 4.

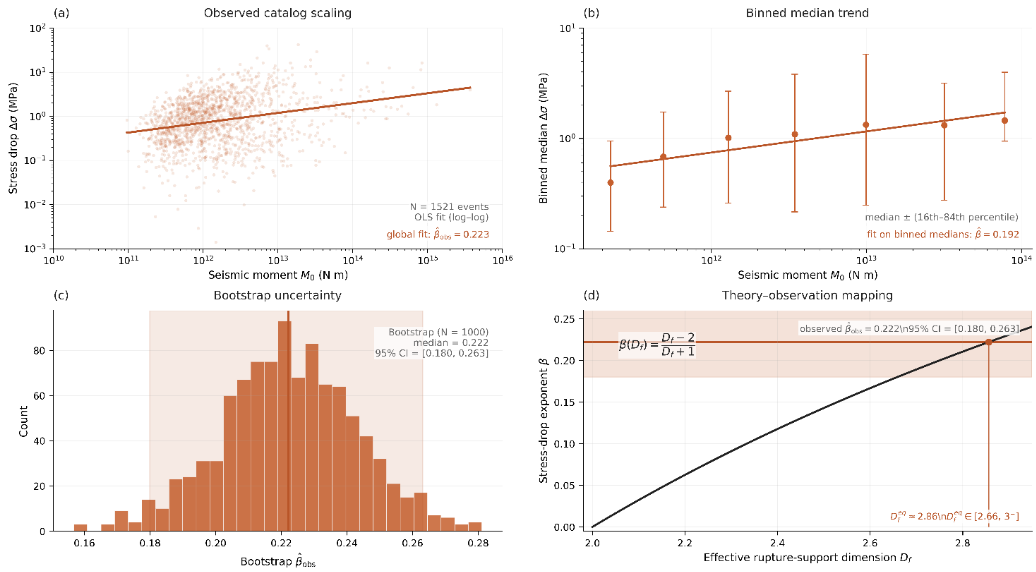

Figure 4. *Observed stress-drop scaling in the Southeastern Alps source-parameter catalog. (a) Static stress drop $\Delta\sigma$ as a function of seismic moment $M_0$for the filtered working catalog, shown in log–log space together with the ordinary least squares fit used to estimate the observational scaling exponent. (b) Binned median $\Delta\sigma$ as a function of M_0; vertical bars indicate the 16th–84th percentile range within each logarithmic moment bin, and the fitted trend to the bin medians provides an independent diagnostic of the catalog-scale scaling. (c) Bootstrap distribution of the observational exponent $\hat{\beta}_{obs}$ based on $N = 1000$ non-parametric resamples; the vertical line marks the bootstrap median and the shaded interval denotes the 95 % confidence interval. (d) Mapping of the observed exponent onto the theoretical relation $\beta(D_f) = (D_f - 2)/(D_f + 1)$. The observational constraint corresponds to an equivalent effective rupture-support dimension D_f^{eq} within the physically admissible interval $2 < D_f < 3$, supporting compatibility between the observed positive stress-drop scaling and a non-Euclidean effective rupture-support interpretation.*

https://doi.org/10.5194/egusphere-2026-3994
Preprint. Discussion started: 5 August 2026

I further evaluated the stability of the inferred exponent using three robustness tests. First, I repeated the regression after imposing progressively higher lower-moment thresholds,

$$\log_{10} M_0^{\min} = 11.0, 11.5, 12.0, 12.5, 13.0. \qquad (26)$$

These thresholds retained approximately $N = 1519$, 1373, 838, 381, and 149 events, respectively. For each threshold, $\hat{\beta}$ was recomputed and uncertainty was estimated by bootstrap resampling. This test evaluates whether the observed scaling is stable across the sampled moment range or instead dominated by the smallest events.

Second, I inspected the residuals of the log–log fit,

$$r_i = y_i - (\hat{a} + \hat{\beta} x_i), \qquad (27)$$

as a function of M_0. A running median of r_i was used to identify systematic curvature or scale-dependent model misfit. The absence of strong residual curvature supports the use of a first-order power-law model over the sampled range, whereas systematic curvature would indicate that a single exponent β is insufficient.

Third, I performed a leave-one-block-out jackknife test. The catalog was partitioned into five subsets constructed to preserve, as far as possible, the overall moment distribution within each block. I then removed one block at a time, refitted Eq. (21), and estimated uncertainty within each retained subset by bootstrap resampling. This procedure evaluates whether the full-catalog estimate is controlled by a specific subset of events.

The analysis therefore combines four complementary estimators or diagnostics: the full-catalog OLS slope, the binned median slope, non-parametric bootstrap uncertainty, and robustness tests based on moment thresholds, residual structure, and subset deletion. The methodological objective is not to infer a unique geometrical dimension directly from individual earthquakes, but to test whether the observed first-order scaling of $\Delta\sigma$ with M_0 is statistically stable and compatible with the theoretical relation derived in Sect. 2.

https://doi.org/10.5194/egusphere-2026-3994
Preprint. Discussion started: 5 August 2026

5 Results

The theoretical framework developed in Sect. 2 predicts that deviations from Euclidean rupture-area scaling should appear as a systematic departure from constant stress drop in log–log $\Delta\sigma$–M_0 space. The conceptual implication is summarized in Fig. 1: a smooth planar rupture support leads to $A \propto L^2$, $M_0 \propto L^3$, and $\Delta\sigma =$ const., whereas a geometrically complex effective rupture support with $A_{\mathrm{eff}} \propto L^{D_f}$ leads to $\Delta\sigma \propto M_0^{\beta}$ for self-similar slip. This contrast defines the observational test performed below.

The analytical dependence of $\Delta\sigma$ on M_0 is shown in Fig. 2 for representative values of the effective rupture-support dimension D_f. For $D_f = 2$, the predicted scaling exponent is $\beta = 0$, and the stress drop is scale invariant. For $D_f > 2$, the curves acquire progressively larger positive slopes, but the predicted exponents remain moderate over the physically admissible interval $2 < D_f < 3$. In particular, the mapping

$$\beta(D_f) = \frac{D_f - 2}{D_f + 1} \qquad (28)$$

implies that even D_f values close to the upper bound of the admissible interval produce $\beta < 0.25$. This result is important because it indicates that the expected signal is not a large departure from constant stress drop, but a weak positive scaling that can be obscured by the substantial scatter typical of stress-drop estimates.

The synthetic experiments in Fig. 3 show that such weak positive scaling is nevertheless recoverable under controlled conditions. Synthetic catalogs generated with prescribed values of β_{true} reproduce the expected log–log trends despite the imposed lognormal scatter. For $\beta_{\mathrm{true}} = 0$, the recovered slopes are centered near zero, whereas positive input exponents yield positive recovered values. The Monte Carlo distributions remain well separated for the tested values $\beta_{\mathrm{true}} = 0.00$, 0.08, and 0.16, indicating that the recovery procedure can distinguish constant-stress-drop behavior from weak geometry-driven scaling for catalog sizes and scatter levels comparable to those used here. The input–output comparison further shows that the median recovered exponent follows the one-to-one reference over the tested interval $0 \leq \beta_{\mathrm{true}} \leq 0.20$. This result does not validate the physical model by itself, but it establishes that the predicted range of β is statistically recoverable under realistic observational scatter.

https://doi.org/10.5194/egusphere-2026-3994
Preprint. Discussion started: 5 August 2026

The observational analysis of the Southeastern Alps catalog is shown in Fig. 4. After filtering for finite and positive M_0 and $\Delta\sigma$, the working catalog contains $N = 1521$ events. The full-catalog log–log regression gives

$$\hat{\beta}_{\mathrm{obs}} = 0.223, \qquad (29)$$

indicating a positive first-order scaling of static stress drop with seismic moment. The fitted relation can therefore be written as

$$\Delta\sigma \propto M_0^{0.223}. \qquad (30)$$

The binned-median analysis provides an independent diagnostic of the trend. Regression of the median stress drop in logarithmic moment bins gives a lower but consistent exponent,

$$\hat{\beta}_{\mathrm{bin}} \simeq 0.192, \qquad (31)$$

showing that the positive trend is not solely controlled by the density structure of the full event cloud. The difference between the event-level and binned estimates is expected because binning reduces the influence of densely sampled portions of the catalog and emphasizes the central tendency within each moment interval. Bootstrap resampling confirms that the positive exponent is stable under repeated sampling of the catalog. The bootstrap distribution of the observational exponent has median

$$\tilde{\beta}_{\mathrm{boot}} = 0.222, \qquad (32)$$

with a 95 % confidence interval

$$0.180 \leq \beta_{\mathrm{obs}} \leq 0.263. \qquad (33)$$

https://doi.org/10.5194/egusphere-2026-3994
Preprint. Discussion started: 5 August 2026

Within the adopted regression and bootstrap model, this interval does not include the Euclidean value $\beta = 0$. The observational result is therefore not consistent with the constant-stress-drop limit under the present assumptions. This statement should be interpreted statistically and conditionally: it refers to the fitted catalog, the adopted source parameters, and the log–log scaling model, not to an absolute exclusion of all Euclidean rupture physics.

Mapping the observed exponent onto the self-similar theoretical relation gives an equivalent effective rupture-support dimension

$$D_f^{\mathrm{eq}} = \frac{2+\beta_{\mathrm{obs}}}{1-\beta_{\mathrm{obs}}}. \qquad (34)$$

Using the bootstrap median exponent yields

$$D_f^{\mathrm{eq}} \simeq 2.86. \qquad (35)$$

The lower bound of the 95 % confidence interval maps to approximately $D_f^{\mathrm{eq}} \simeq 2.66$, whereas the upper bound approaches the physical limit $D_f \to 3^-$. Consequently, the observationally compatible range is approximately

$$D_f^{\mathrm{eq}} \in [2.66, 3^-]. \qquad (36)$$

The nonlinear nature of this inverse mapping is important: uncertainty in β is amplified as D_f^{eq} approaches 3. Therefore, the most robust inference is not the exact numerical value of D_f^{eq}, but the fact that the observed positive exponent maps into the non-Euclidean admissible regime $2 < D_f < 3$.

https://doi.org/10.5194/egusphere-2026-3994
Preprint. Discussion started: 5 August 2026

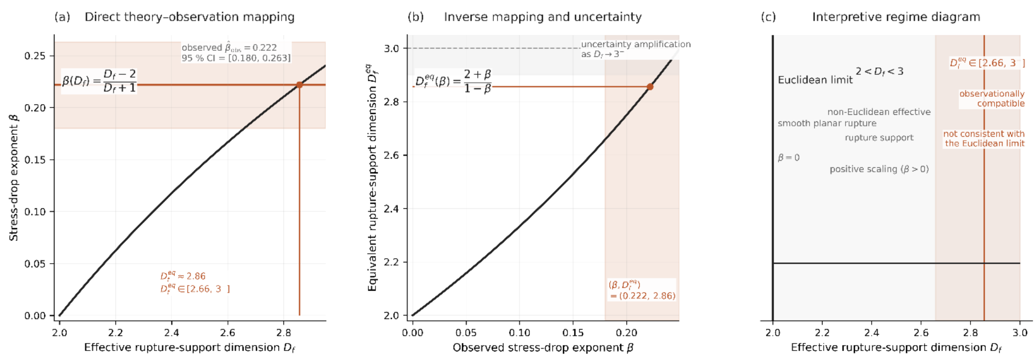

Figure 5. *Physical interpretation of the observed stress-drop scaling within the effective rupture-support framework. (a) Direct theoretical mapping between the effective rupture-support dimension D_f and the stress-drop scaling exponent β, with the observational constraint from Fig. 4 superimposed. The observed median exponent maps to an equivalent dimension D_f^{eq}, while the shaded band indicates the bootstrap uncertainty range. (b) Inverse mapping from $\beta$to $D_f^{eq} = (2+\beta)/(1-\beta)$, showing the nonlinear amplification of uncertainty as the inferred equivalent dimension approaches the upper bound $D_f = 3$. (c) Interpretive regime diagram summarizing the Euclidean limit $(D_f = 2)$, the physically admissible non-Euclidean interval $(2 < D_f < 3)$, and the range compatible with the observational estimate. Together, the panels show that the observed positive stress-drop scaling is compatible with a geometrically complex effective rupture support and is not consistent with the smooth-planar Euclidean limit under the adopted scaling and uncertainty model.*

Figure 5 provides the physical interpretation of this mapping. The direct relation $\beta(D_f)$ places the observational constraint within the fractal-compatible interval, while the inverse mapping $D_f^{\mathrm{eq}}(\beta)$ shows the increasing sensitivity of equivalent dimension estimates near the upper bound. The regime diagram summarizes three distinct domains: the Euclidean limit $D_f = 2$, the physically admissible non-Euclidean interval $2 < D_f < 3$, and the observationally compatible range inferred from the Southeastern Alps catalog. The consolidated result is that the observed scaling is compatible with a geometrically complex effective rupture support. The more cautious interpretation is that the inferred D_f^{eq} is a model-dependent proxy for rupture-support complexity, not a direct geometrical measurement.

https://doi.org/10.5194/egusphere-2026-3994
Preprint. Discussion started: 5 August 2026

The robustness tests in Fig. 6 evaluate whether the positive exponent is controlled by threshold choice, residual structure, or a restricted subset of events. Repeating the regression for increasing lower-moment thresholds shows that the recovered $\hat{\beta}$ remains positive across the tested thresholds. The estimates vary as the retained sample size decreases, with the strongest instability occurring at the highest threshold, where only $N \simeq 149$ events remain. This behavior indicates that high-threshold estimates are affected by reduced statistical support rather than by a systematic collapse of the positive scaling.

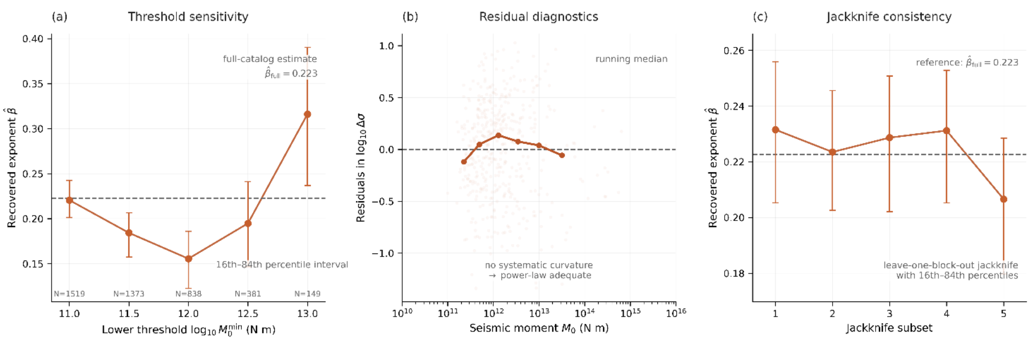

Figure 6. *Robustness tests for the observed stress-drop scaling in the Southeastern Alps catalog. (a) Sensitivity of the recovered scaling exponent $\hat{\beta}$ to the lower moment threshold $log_{10}M_0^{min}$. Points indicate bootstrap medians, and vertical bars denote the 16th–84th percentile range; labels near the lower axis report the number of events retained at each threshold. The dashed horizontal line marks the full-catalog estimate $\hat{\beta}_{full} = 0.223$. The exponent remains positive across the tested thresholds, with the largest deviations occurring where the retained sample size is strongly reduced. (b) Residuals of the log–log power-law fit as a function of seismic moment. The running median remains close to zero over most of the populated moment range, indicating no strong systematic curvature and supporting the use of a first-order power-law approximation. (c) Leave-one-block-out jackknife test using partitions designed to preserve the moment distribution. Points show median $\hat{\beta}$ values with 16th–84th percentile bootstrap intervals, and the dashed line again marks the full-catalog estimate. The jackknife estimates remain consistent with $\hat{\beta}_{full}$, indicating that the inferred positive scaling is not controlled by a single subset of events.*

https://doi.org/10.5194/egusphere-2026-3994
Preprint. Discussion started: 5 August 2026

Residual diagnostics further support the use of a first-order power-law model over the sampled range. The residuals of the log–log regression do not show strong systematic curvature as a function of seismic moment, and the running median remains close to zero over most of the populated moment interval. This does not imply that the model captures all source complexity, but it indicates that a single exponent provides an adequate first-order description of the catalog-scale trend.

The leave-one-block-out jackknife test provides an additional check on subset dependence. Removing each moment-preserving block in turn yields $\hat{\beta}$ estimates that remain close to the full-catalog value. The jackknife results therefore indicate that the observed positive scaling is not dominated by a single subset of events. Taken together, the threshold analysis, residual diagnostics, and jackknife test support the stability of the inferred exponent within the limitations of the available catalog.

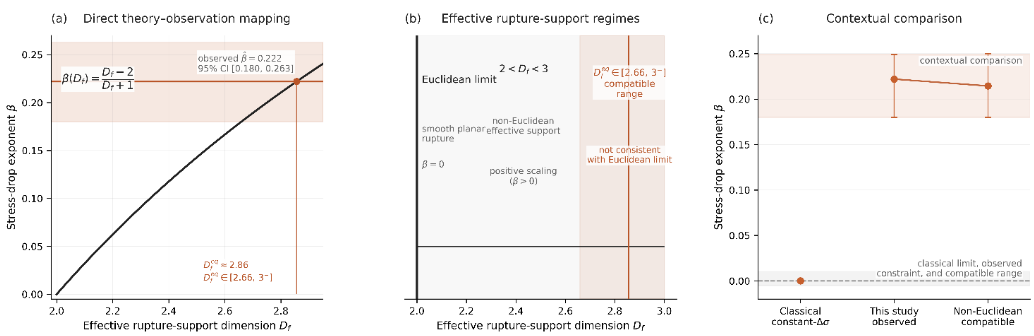

Figure 7. *Physical interpretation and contextualization of the observed stress-drop scaling. (a) Theoretical mapping between the effective rupture-support dimension D_f and the stress-drop exponent β, with the observational constraint from Fig. 4 superimposed. The observed median exponent maps to an equivalent dimension D_f^{eq} within the non-Euclidean effective-support regime. (b) Interpretive regime diagram showing the Euclidean limit $(D_f = 2)$, the physically admissible non-Euclidean interval $(2 < D_f < 3)$, and the range compatible with the observational estimate. The shaded observational interval indicates that the inferred scaling is not consistent with the smooth-planar Euclidean limit under the adopted model assumptions. (c) Contextual comparison between the classical constant-stress-drop limit ($\beta = 0$), the observational estimate obtained in this study, and the theoretically admissible non-Euclidean scaling range. The observed positive exponent supports compatibility with a geometrically complex effective rupture support, while remaining*

https://doi.org/10.5194/egusphere-2026-3994
Preprint. Discussion started: 5 August 2026

conditional on self-similar slip, homogeneous source-parameter estimation, and the absence of unresolved scale-dependent bias.

Figure 7 contextualizes the observational result relative to the Euclidean and non-Euclidean regimes. The classical constant-stress-drop paradigm corresponds to $\beta = 0$and $D_f = 2$. The observed estimate lies at positive β, within the interval predicted for $2 < D_f < 3$. The result therefore supports the interpretation that the source-parameter catalog is more consistent with an effective rupture support of non-Euclidean dimension than with the smooth-planar limit. This conclusion is conditional on the assumptions of self-similar slip and homogeneous source-parameter estimation.

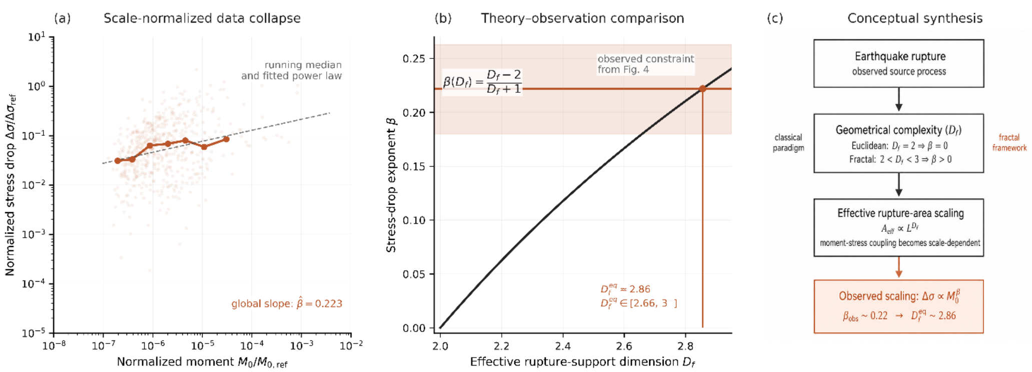

Figure 8. *Unified scaling synthesis and physical implications. (a) Scale-normalized $\Delta\sigma$–M_0 data collapse for the Southeastern Alps source-parameter catalog. The running median shows the central tendency of the normalized observations, while the dashed reference trend represents the fitted power-law scaling $\Delta\sigma \propto M_0^{\beta}$. (b) Comparison between the theoretical mapping $\beta(D_f) = (D_f - 2)/(D_f + 1)$and the observational constraint from Fig. 4. The observed positive exponent maps, under self-similar slip, to an equivalent rupture-support dimension $D_f^{eq} \approx 2.86$, within the admissible non-Euclidean interval $2 < D_f < 3$. (c) Conceptual synthesis linking rupture geometry to observable stress-drop scaling. In the proposed framework, increasing effective rupture-support complexity modifies the rupture-area scaling, $A_{eff} \propto L^{D_f}$, and leads to scale-dependent stress-drop behavior. The observed scaling is therefore compatible with a geometrically complex*

https://doi.org/10.5194/egusphere-2026-3994
Preprint. Discussion started: 5 August 2026

effective rupture support and departs from the classical constant-stress-drop expectation under the adopted model assumptions.

Finally, Fig. 8 synthesizes the scaling result and its physical implication. The normalized data collapse shows that the observed stress-drop values follow a coherent power-law trend over multiple decades in seismic moment, although with substantial scatter. The theoretical comparison places the observed exponent on the $\beta(D_f)$ curve, and the conceptual synthesis links the chain of inference from rupture geometry to effective rupture-area scaling and then to observable stress-drop scaling. The principal empirical result is therefore a robust positive stress-drop exponent,

$$\beta_{\mathrm{obs}} \simeq 0.22, \qquad (37)$$

which maps, under self-similar slip, to

$$D_f^{\mathrm{eq}} \simeq 2.86. \qquad (38)$$

The principal physical interpretation is that the observed scaling is compatible with a geometrically complex effective rupture support. The speculative extension, to be tested with independent finite-source or structural data, is that the equivalent dimension inferred from stress-drop scaling reflects the multiscale geometry of the active rupture network.

6 Discussion

The principal result of this study is that the Southeastern Alps source-parameter catalog exhibits a positive first-order scaling of static stress drop with seismic moment. The full-catalog estimate, $\hat{\beta}_{\mathrm{obs}} = 0.223$, the binned-median estimate, $\hat{\beta}_{\mathrm{bin}} \simeq 0.192$, and the bootstrap median, $\tilde{\beta}_{\mathrm{boot}} = 0.222$, are mutually consistent within the adopted uncertainty framework. The 95 % bootstrap confidence interval, $0.180 \leq \beta_{\mathrm{obs}} \leq 0.263$,

https://doi.org/10.5194/egusphere-2026-3994
Preprint. Discussion started: 5 August 2026

does not include the Euclidean value $\beta = 0$. Within the regression model used here, the observational trend is therefore not consistent with the classical constant-stress-drop limit. This result is the consolidated empirical outcome of the analysis.

The theoretical framework provides a direct interpretation of this positive exponent. If slip is self-similar, $\alpha = 1$, and the effective rupture support scales as $A_{\mathrm{eff}} \propto L^{D_f}$, then the predicted stress-drop exponent is

$$\beta = \frac{D_f - 2}{D_f + 1}. \qquad (39)$$

Under this mapping, the observed exponent corresponds to an equivalent effective rupture-support dimension of approximately

$$D_f^{\mathrm{eq}} \simeq 2.86. \qquad (40)$$

The observationally compatible interval, approximately $D_f^{\mathrm{eq}} \in [2.66, 3^{-}]$, lies within the physically admissible non-Euclidean range $2 < D_f < 3$. The plausible physical interpretation is therefore that the observed stress-drop scaling reflects an effective rupture support whose geometrical complexity increases with source size. This interpretation is consistent with the broader evidence that natural faults and fault systems display scale-dependent roughness, segmentation, and fractal or self-affine geometrical properties over finite observational ranges (Brown and Scholz, 1985; Power et al., 1987; Okubo and Aki, 1987).

The result does not imply that earthquake ruptures in the Southeastern Alps occupy a literal volumetric domain. The exponent D_f^{eq} should instead be interpreted as an effective dimension of the active rupture support. This distinction is critical. A mapped fault surface, a distributed rupture network, and a catalog-inferred effective support are not identical geometrical objects. The present analysis does not directly image rupture geometry; it infers a scaling exponent from source parameters and maps that exponent onto a theoretical geometrical relation. Thus, the robust inference is that the stress-drop scaling is compatible with a non-Euclidean effective support. The stronger statement that D_f^{eq} directly measures the fractal dimension of the active rupture network

https://doi.org/10.5194/egusphere-2026-3994
Preprint. Discussion started: 5 August 2026

remains speculative and requires independent validation from finite-source inversions, high-resolution relocated seismicity, fault-trace geometry, or dynamic rupture simulations.

The positive value of β_{obs} is also physically meaningful because the predicted exponents are expected to be moderate. Equation (39) implies $0 < \beta < 1/4$for $2 < D_f < 3$. Consequently, the observed value near 0.22 is close to the upper part of the admissible interval but does not exceed it. This position explains both the strength and the limitation of the result. On one hand, the exponent is sufficiently positive to be statistically separated from the Euclidean limit in the analyzed catalog. On the other hand, the inverse mapping becomes increasingly sensitive as D_f^{eq} approaches 3. Small changes in βnear the upper bound produce large changes in D_f^{eq}. For this reason, the exact numerical value $D_f^{\mathrm{eq}} \simeq 2.86$ should not be overinterpreted. The more stable conclusion is that the observed exponent maps into the non-Euclidean regime.

The synthetic tests are important for interpreting the observational result. Stress-drop estimates are known to show large scatter because they depend on corner frequency, attenuation correction, source model assumptions, bandwidth, path effects, and site effects. The synthetic experiments demonstrate that exponents in the range predicted by the framework remain recoverable under lognormal scatter comparable to that expected for source-parameter estimates. This does not eliminate methodological uncertainty in the observational catalog, but it shows that a weak positive exponent is not automatically undetectable. The synthetic tests therefore support the statistical identifiability of the signal, while the observational robustness tests address its catalog dependence.

The robustness analysis indicates that the positive exponent is not controlled by a single methodological choice. The threshold test shows that $\hat{\beta}$ remains positive over a broad range of lower-moment cutoffs. Instability increases only at the highest threshold, where the retained sample size is strongly reduced. The residual analysis does not show strong systematic curvature in log–log space, supporting a first-order power-law approximation over the sampled moment range. The leave-one-block-out jackknife further indicates that the full-catalog estimate is not dominated by a single subset of events. Taken together, these diagnostics support the stability of the observed scaling within the available catalog.

Nevertheless, several alternative explanations must be considered. First, the observed positive exponent may be influenced by unresolved trade-offs among seismic moment, corner frequency, source radius, and static

https://doi.org/10.5194/egusphere-2026-3994
Preprint. Discussion started: 5 August 2026

stress drop. In spectral source analysis, $\Delta\sigma$ is not an independent direct observable; it is derived from source-size estimates, which are themselves sensitive to corner-frequency measurement and attenuation correction. A systematic dependence of corner-frequency bias on event size could therefore induce an apparent stress-drop scaling. Second, catalog selection effects may affect the low-moment range, where detection, signal-to-noise ratio, bandwidth, and quality-control thresholds can influence the retained sample. Third, the regional tectonic setting may contribute to the observed scaling. The Southeastern Alps are structurally heterogeneous, and the inferred exponent may reflect a regional mixture of source processes rather than a universal earthquake property. These alternatives do not invalidate the framework, but they constrain the strength of the interpretation.

The distinction between consolidated results, plausible interpretations, and speculative extensions is therefore central. The consolidated result is that the analyzed catalog shows a stable positive $\Delta\sigma$–M_0 exponent. The plausible interpretation is that this exponent is compatible with an effective rupture-support geometry more complex than a smooth Euclidean plane. The speculative extension is that the equivalent dimension inferred from stress-drop scaling approximates the fractal dimension of the active rupture network. Only the first statement is directly demonstrated by the data. The second follows from the theoretical framework under the stated assumptions. The third requires independent geometrical evidence.

This framework also clarifies why apparent deviations from constant stress drop should not be treated only as noise or methodological artifact. In the classical Euclidean model, constant stress drop follows from the simultaneous assumptions $A \propto L^2$, $\bar{u} \propto L$, and $M_0 \propto L^3$(Aki, 1967; Brune, 1970; Kanamori and Anderson, 1975). If the effective rupture support departs from L^2scaling, then scale-dependent stress drop is not anomalous; it is an expected consequence of geometrical scaling. The present formulation therefore provides a physically interpretable mechanism by which fault complexity can enter source-parameter scaling without abandoning the moment definition or the first-order stress-drop relation.

A key implication is that stress-drop scaling may encode information about rupture-support geometry, but only in an effective and model-dependent sense. The same observed exponent may result from different combinations of D_f and α, as shown by the general relation

https://doi.org/10.5194/egusphere-2026-3994
Preprint. Discussion started: 5 August 2026

$$\beta = \frac{D_f + \alpha - 3}{D_f + \alpha}. \qquad (41)$$

The self-similar assumption $\alpha = 1$ is useful because it yields a closed mapping between β and D_f^{eq}, but it is not the only admissible physical possibility. If average slip scales differently from L, part of the observed positive exponent may be attributed to slip scaling rather than rupture-support geometry. Future work should therefore attempt to constrain α independently using finite-source models or source-radius estimates. This would allow Eq. (41) to be used in its general form rather than relying on the self-similar reduction.

The regional nature of the observational test is another important limitation. The theoretical model is general, but the empirical evidence presented here is based on a single open catalog from the Southeastern Alps. The result should therefore not be described as global evidence for fractal rupture scaling. A stronger claim would require independent tests in multiple tectonic settings, including continental strike-slip regions, normal-faulting sequences, subduction interfaces, induced seismicity, and volcanic or geothermal environments. Such tests should use catalogs in which M_0, corner frequency, and stress drop are estimated with internally consistent procedures. Comparisons among regions would then allow one to determine whether β and D_f^{eq} are stable source-scaling properties or region-specific descriptors of fault-zone structure and catalog methodology.

The framework is particularly suitable for such comparative applications because it makes a simple, falsifiable prediction. If an internally homogeneous source-parameter catalog yields $\beta \simeq 0$, then the data are compatible with Euclidean self-similar rupture scaling. If a robust positive $\beta$is recovered and cannot be explained by methodological bias, then the data are compatible with non-Euclidean effective rupture-support scaling. If β exceeds the theoretical upper bound implied by $2 < D_f < 3$ under self-similar slip, then either the self-similar assumption is invalid, the stress-drop estimates contain scale-dependent bias, or the proposed geometrical model is incomplete. This falsifiability is a strength of the formulation.

The broader contribution of the study is therefore conceptual rather than purely regional. The analysis provides an explicit mathematical bridge between rupture geometry and observable stress-drop scaling. It shows that a moderate positive exponent can arise naturally from an effective support dimension larger than two, and it demonstrates that such an exponent is recoverable and stable in one open source-parameter catalog. The result does not resolve the long-standing debate on whether earthquake stress drop is universally constant, scale

https://doi.org/10.5194/egusphere-2026-3994
Preprint. Discussion started: 5 August 2026

dependent, or regionally variable. Instead, it reframes one possible class of stress-drop scaling observations as a testable consequence of non-Euclidean rupture geometry.

In summary, the Southeastern Alps catalog supports a positive stress-drop scaling exponent that is incompatible with the Euclidean constant-stress-drop limit under the adopted regression and uncertainty model. The exponent maps to an equivalent effective rupture-support dimension within the admissible interval $2 < D_f < 3$, providing a physically consistent interpretation in terms of geometrical rupture complexity. The interpretation remains conditional on self-similar slip, homogeneous source-parameter estimation, and the absence of unmodeled scale-dependent bias. The most defensible conclusion is therefore not that fractal rupture geometry is directly demonstrated, but that the proposed fractal rupture-support framework is mathematically derived, observationally compatible, and robust for the analyzed regional catalog.

7 Conclusions

This study developed and tested a geometrical scaling framework in which earthquake stress-drop scaling emerges from the effective dimension of the rupture support. In the classical Euclidean limit, rupture area scales as $A \propto L^2$, seismic moment scales as $M_0 \propto L^3$, and static stress drop is scale invariant. By replacing the Euclidean rupture area with an effective geometrically complex support, $A_{\text{eff}} \propto L^{D_f}$, the framework predicts a power-law stress-drop scaling, $\Delta\sigma \propto M_0^{\beta}$. For self-similar slip, this gives the analytical relation $\beta = (D_f - 2)/(D_f + 1)$, linking the observable stress-drop exponent to an equivalent rupture-support dimension.

Synthetic tests showed that weak positive exponents in the range predicted by the model are recoverable under realistic lognormal scatter. This result is important because stress-drop estimates are intrinsically variable and sensitive to source-spectral assumptions, attenuation correction, bandwidth, and corner-frequency uncertainty. The synthetic experiments therefore demonstrate that the expected signal is statistically identifiable, although they do not by themselves validate the physical interpretation.

Application to an open source-parameter catalog from the Southeastern Alps yielded a positive observational stress-drop exponent, $\hat{\beta}_{\text{obs}} = 0.223$, with bootstrap median 0.222and 95 % confidence interval $[0.180, 0.263]$. The binned-median estimate, $\hat{\beta}_{\text{bin}} \simeq 0.192$, is consistent with the full-catalog trend. Under the

https://doi.org/10.5194/egusphere-2026-3994
Preprint. Discussion started: 5 August 2026

self-similar slip assumption, the observed exponent maps to an equivalent effective rupture-support dimension $D_f^{\mathrm{eq}} \simeq 2.86$, with an observationally compatible interval approximately $[2.66, 3^{-}]$. Within the adopted regression and uncertainty model, the analyzed catalog is therefore not consistent with the Euclidean constant-stress-drop limit and is compatible with a non-Euclidean effective rupture-support scaling.

Robustness tests support the stability of the inferred exponent. The positive scaling persists across lower-moment thresholds, residual diagnostics do not indicate strong systematic curvature, and leave-one-block-out jackknife tests show that the result is not controlled by a single subset of events. These diagnostics strengthen the empirical result, although they do not eliminate all possible sources of bias. In particular, scale-dependent effects in corner-frequency estimation, attenuation correction, catalog selection, and regional tectonic heterogeneity remain plausible contributors to the observed scaling.

The main contribution of the study is therefore not the claim that fractal rupture geometry is directly observed, but the demonstration that a mathematically derived non-Euclidean rupture-support framework provides a physically consistent and observationally compatible explanation for positive stress-drop scaling in the analyzed regional catalog. The quantity D_f^{eq} should be interpreted as a model-dependent effective dimension, not as a direct measurement of fault fractality. Future tests should apply the same framework to independently processed source-parameter catalogs from multiple tectonic settings and should combine stress-drop scaling with finite-source constraints, relocated seismicity, and mapped fault-zone geometry. Such extensions would determine whether the inferred scaling is a regional property of the Southeastern Alps or a more general feature of earthquake rupture in geometrically complex fault systems.

Code and data availability

The primary observational dataset used in this study is publicly available from Zenodo: *Catalog of source parameters estimated for earthquakes occurred in Southeastern Alps* (Moratto and Saraò, 2025), https://doi.org/10.5281/zenodo.16940390. The dataset contains source parameters for earthquakes that occurred in the Southeastern Alps from 2016 to 2023, including moment magnitude M_W, seismic moment M_0, corner frequency f_c, quality factor Q_0, source radius r, static stress drop $\Delta\sigma$, radiated energy E_r, apparent stress, and seismic efficiency. The source parameters were estimated using the SourceSpec software (Satriano,

https://doi.org/10.5194/egusphere-2026-3994
Preprint. Discussion started: 5 August 2026

2024). The Zenodo record specifies that the dataset is distributed under the Creative Commons Attribution 4.0 International license.

The analysis used only events for which both M_0 and $\Delta\sigma$ were finite and strictly positive, because the regression model is defined in logarithmic space. The filtered working catalog, derived tables, figure-ready data files, and all Python scripts used to reproduce the synthetic experiments, observational regressions, bootstrap analyses, robustness tests, and figures will be deposited in a public Zenodo repository before submission. The repository DOI will be inserted here after deposition:

Code and derived data repository: DOI to be inserted.

All scripts will be provided as standalone Python files requiring only standard scientific Python libraries. The repository will include instructions to reproduce Figs. 1–8 and the numerical values reported in the Results section, including $\hat{\beta}_{\mathrm{obs}}$, the binned-median estimate, bootstrap confidence intervals, moment-threshold sensitivity tests, residual diagnostics, jackknife estimates, and the inferred D_f^{eq} range.

No restricted, confidential, or proprietary data were used in this study.

References

Abercrombie, R. E.: Earthquake source scaling relationships from -1t o $5M_L$ using seismograms recorded at 2.5 km depth, J. Geophys. Res., 100, 24015–24036, https://doi.org/10.1029/95JB02397, 1995.

Allmann, B. P. and Shearer, P. M.: Global variations of stress drop for moderate to large earthquakes, J. Geophys. Res., 114, B01310, https://doi.org/10.1029/2008JB005821, 2009.

Aki, K.: Scaling law of seismic spectrum, J. Geophys. Res., 72, 1217–1231, https://doi.org/10.1029/JZ072i004p01217, 1967.

https://doi.org/10.5194/egusphere-2026-3994
Preprint. Discussion started: 5 August 2026

Brodsky, E. E., Kirkpatrick, J. D., and Candela, T.: Constraints from fault roughness on the scale-dependent strength of rocks, Geology, 44, 19–22, https://doi.org/10.1130/G37206.1, 2016.

Brown, S. R. and Scholz, C. H.: Broad bandwidth study of the topography of natural rock surfaces, J. Geophys. Res., 90, 12575–12582, https://doi.org/10.1029/JB090iB14p12575, 1985.

Brune, J. N.: Tectonic stress and the spectra of seismic shear waves from earthquakes, J. Geophys. Res., 75, 4997–5009, https://doi.org/10.1029/JB075i026p04997, 1970.

Candela, T., Renard, F., Klinger, Y., Mair, K., and Schmittbuhl, J.: Roughness of fault surfaces over nine decades of length scales, J. Geophys. Res., 117, B08409, https://doi.org/10.1029/2011JB009041, 2012.

Efron, B.: Bootstrap methods: another look at the jackknife, Ann. Stat., 7, 1–26, https://doi.org/10.1214/aos/1176344552, 1979.

Ide, S. and Beroza, G. C.: Does apparent stress vary with earthquake size?, Geophys. Res. Lett., 28, 3349–3352, https://doi.org/10.1029/2001GL013106, 2001.

Kanamori, H. and Anderson, D. L.: Theoretical basis of some empirical relations in seismology, Bull. Seismol. Soc. Am., 65, 1073–1095, https://doi.org/10.1785/BSSA0650051073, 1975.

Okubo, P. G. and Aki, K.: Fractal geometry in the San Andreas fault system, J. Geophys. Res., 92, 345–355, https://doi.org/10.1029/JB092iB01p00345, 1987.

Moratto, L. and Saraò, A.: Catalog of source parameters estimated for earthquakes occurred in Southeastern Alps, Zenodo [data set], https://doi.org/10.5281/zenodo.16940390, 2025.

https://doi.org/10.5194/egusphere-2026-3994
Preprint. Discussion started: 5 August 2026

Moratto, L., Abdi, F., and Saraò, A.: Seismic source parameters analysis in Southeastern Alps and associated tectonic implications, Tectonophysics, 923, 231069, https://doi.org/10.1016/j.tecto.2026.231069, 2026.

Power, W. L., Tullis, T. E., Brown, S. R., Boitnott, G. N., and Scholz, C. H.: Roughness of natural fault surfaces, Geophys. Res. Lett., 14, 29–32, https://doi.org/10.1029/GL014i001p00029, 1987.

Satriano, C.: SourceSpec – Earthquake source parameters from P- or S-wave displacement spectra (1.8), Zenodo [software], https://doi.org/10.5281/zenodo.3688587, 2024.